

Collective conical intersections through light-matter coupling in a cavity

Oriol Vendrell^{1,*}

¹*Department of Physics and Astronomy, Aarhus University, Ny Munkegade 120, 8000 Aarhus C, Denmark*
(Dated: December 14, 2024)

The photo-triggered dynamics and non-radiative relaxation pathways of a molecular ensemble coupled to a resonance cavity are considered theoretically. In the one-molecule and single excitation limits, the coupling of a vibrationally bound electronic ground state and a dissociative excited state result in a lower polariton state with dissociative character and an upper polariton supporting long-lived vibronic-polaritonic resonances. As the number of molecules increases, dark light-matter states appear between the two optically active polaritons. These dark states feature a rich structure of true collective conical intersection crossings, whose location depends on the internal atomic coordinates of each molecule in the ensemble, and which lead to ultrafast non-radiative decay from the upper polariton. At least three coupled molecules are necessary for cavity-induced collective conical intersections to exist and, for identical coupled molecules, they constitute a special case of Jahn-Teller-type electronic state intersections. It is argued that the existence of this kind of conical intersection explains the ultrafast non-radiative decay in cavities observed in recent experiments.

The interaction of atoms and molecules with quantized light has the potential to open new routes towards manipulating their physical and chemical properties, and towards the development of hybrid matter-light systems with new attributes [1–6]. Over the past few years ground breaking experiments on those kinds of systems [7–11] have demonstrated the effective tuning of reaction rates and probabilities [9], energy transfer rates among different molecular species [12] and of the vibrational properties of molecules [13, 14]. A growing body of theory results [13, 15–28] has lead, among others, to propose mechanisms to suppress [20] or catalyze chemical processes [25] through the cavity mode, to modify the non-adiabatic dynamics of a single molecule in a cavity [22], and to model the mechanism of inter-molecular energy transfer among different molecular species in a cavity [28].

Experimentally, it has been observed that photo-excitation of the upper polariton branch (UPB) in a coupled cavity-matter system is followed by population transfer to the lower polariton branch (LPB) before light emission from the UPB can take place [7, 10]. Time-resolved measurements in hybrid organic dye-molecule systems indicate that population transfer from the UPB to the LPB occurs within a time-scale of tens to hundreds of femtoseconds [10], orders of magnitude shorter than the radiative life-time of the molecular excited states in isolation. The fast relaxation time-scale in presence of a cavity suggests the involvement of a collective mechanism that funnels population from the UPB to the LPB, where thereafter, e.g., spontaneous photon emission or a chemical reaction can occur.

The simulation of a molecular ensemble coupled to a cavity has been recently achieved by a mixed quantum-classical approach with classical nuclei, which could explain some aspects of the non-radiative decay large molecules in the cavity [26]. On the other hand, full, real-time quantum dynamics descriptions require approaches that can overcome the course of dimensionality with in-

creasing numbers of intra-molecular degrees of freedom and of coupled molecules [27]. In this work, numerically converged quantum dynamics simulations of a molecular ensemble coupled to resonance cavity and theoretical considerations are used to explain the underlying collective mechanisms resulting in the ultrafast non-radiative decay dynamics experience by the hybrid system. It is shown that this mechanism is of vibronic origin and related to the existence of cavity-induced collective conical intersections (CCI).

An ensemble of diatomic molecules aligned with the polarization axis of the cavity mode is considered. The molecules are assumed to not interact directly with one another. The Hamiltonian for the molecular ensemble and cavity reads

$$\hat{H} = \hat{T}_n + \hat{H}_{\text{el}} + \hat{H}_{\text{cav}} + \hat{H}_{\text{las}}, \quad (1)$$

where $\hat{T} = \sum_{\kappa}^N \hat{t}_n^{(\kappa)}$ is the sum of nuclear kinetic energy operators for each κ -th molecule, $\hat{H}_{\text{el}} = \sum_{\kappa}^N \hat{h}_{\text{el}}^{(\kappa)}$ is the sum of all other intramolecular Hamiltonian terms for each molecule

$$\hat{h}_{\text{el}}^{(\kappa)} = \hat{t}_e^{(\kappa)} + \hat{v}_{ee}^{(\kappa)} + \hat{v}_{en}^{(\kappa)} + \hat{v}_{nn}^{(\kappa)}, \quad (2)$$

\hat{H}_{cav} is the cavity and cavity-ensemble Hamiltonian, and \hat{H}_{las} describes the coupling to an external laser field. The terms in Eq. (2) correspond to the κ -th electronic kinetic energy and the Coulombic terms represent the electron-electron repulsion, electron-nuclei attraction and nuclei-nuclei repulsion, respectively. The cavity Hamiltonian is given by [17, 24, 27, 29]

$$\hat{H}_{\text{cav}} = \hbar\omega_c \left(\frac{1}{2} + \hat{a}^\dagger \hat{a} \right) + g \vec{\epsilon}_c \cdot \vec{D} (\hat{a}^\dagger + \hat{a}), \quad (3)$$

where ω_c is the angular frequency of the cavity mode, $\vec{\epsilon}_c$ is the polarization direction of the cavity, and $g = \sqrt{\hbar\omega_c/2V\epsilon_0}$ is the coupling strength between the

cavity and the molecules. V is the quantization volume of the cavity mode and also the physical volume of the cavity. $\vec{D} = \sum_{\kappa}^N \vec{\mu}^{(\kappa)}$ is total dipole operator of the ensemble. In Eq. (3), the quadratic dipole self-energy term is being neglected, which is only relevant at much higher coupling strengths than considered here. For further details see, e.g., Refs. [24, 29]. The coupling of an external laser field to the molecular ensemble is introduced semi-classically in the length gauge and dipole approximation as $\hat{H}_{\text{las}} = -\vec{E}(t)\vec{D}$, where the electric field takes the form $\vec{E}(t) = \vec{\epsilon}_L A(t) \cos(\omega_L t)$. Here it is assumed that an external laser, if present, couples exclusively to the molecules and not to the cavity. This is motivated by the assumption that the laser field propagates perpendicularly to the propagation direction of the cavity photons, such that the direct coupling of the laser and the cavity mode is minimized [16, 27].

As an illustrative molecular example we consider sodium iodide (NaI), whose ultrafast photo-dissociation dynamics in the first excited electronic state 1A coupled to the ground electronic state 1X has been the subject of extensive experimental and theoretical investigations (cf. Ref. [30]), also in the context of cavity-induced chemistry [22, 27]. Details on the potential energy and transition dipole curves of NaI [27] and a detailed account of the quantum dynamics numerical techniques employed in this work can be found elsewhere [27, 31, 32].

Photo-excitation of an isolated NaI molecule results in its immediate dissociation in the electronic excited potential energy surface. The corresponding absorption spectrum features therefore a single absorption band of, in this case, full width at half maximum (fwhm) of about 0.2 eV centered at an excitation energy of about 3.7 eV, which is seen in the right panel in Fig. (1a). The absorption spectrum $\sigma(\omega) \propto \Re\{\omega \int_0^\infty e^{i\omega t} a(t) dt\}$ is computed from the dipole auto-correlation function $a(t) = \langle \Psi_\mu(0) | e^{-i\hat{H}t/\hbar} | \Psi_\mu(0) \rangle$, where $|\Psi_\mu(0)\rangle = \vec{\epsilon}_L \cdot \vec{D} |\Psi_0\rangle$ and $|\Psi_0\rangle$ is the absolute ground state of the system. The strongly dissociative potential energy surface of the first excited electronic state responsible for the fast dissociation is shown in the left panel of Fig. (1a), where the ground state potential energy surface shifted by the cavity photon energy $V_0(R) + \frac{3}{2}\hbar\omega_c$ is shown as a dashed curve for comparison.

The red dots in the right panel of Fig. (1a) indicate the dissociation probability of the NaI molecule when excited with a z -polarized 30 fs laser pulse (fwhm) of the corresponding photon energy and a peak field amplitude of $5 \cdot 10^{-4}$ au. This relatively weak field ensures that the light absorption takes place in the linear regime and hence the only relevant process is single photon absorption into the single excitation space. For the chosen laser parameters, the dissociation probability at the center of the absorption band is slightly larger than 10%. For an

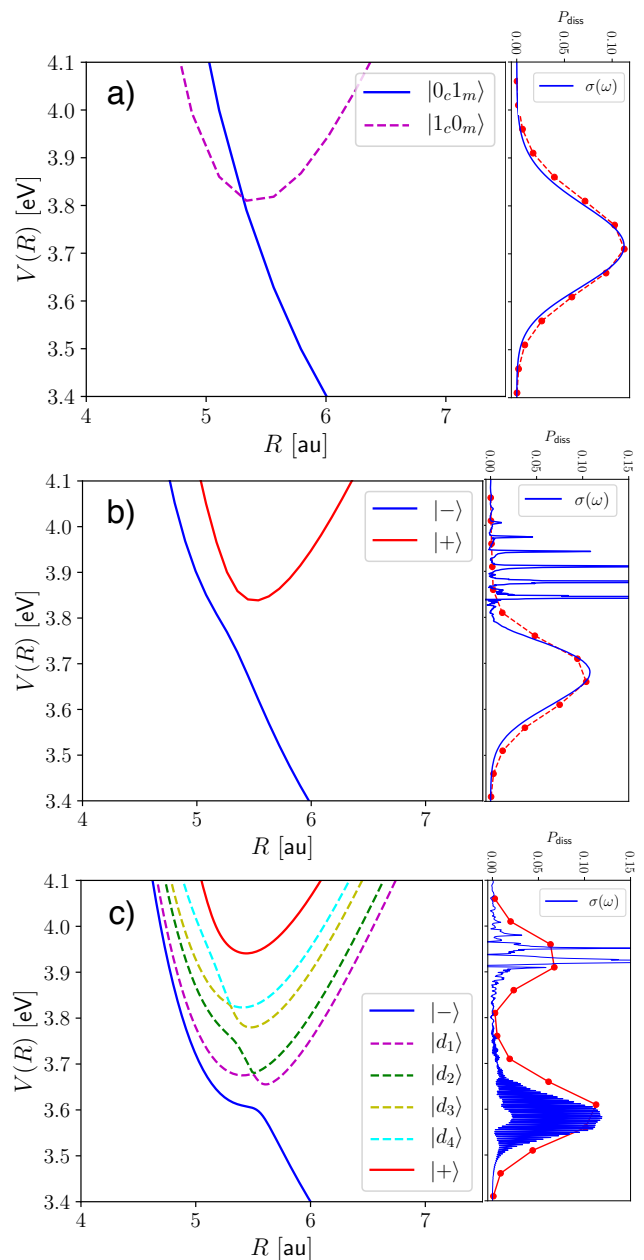


FIG. 1. Left panels: one-dimensional cuts along adiabatic polaritonic potential energy surfaces obtained by diagonalization of $\mathcal{H}_{\text{el-cav}}^{[1]}(\mathbf{R})$ (cf. Eq. (4)). Right panels: absorption spectrum of the hybrid system (blue solid curves) and single-molecule photo-dissociation probability at the corresponding photon-energy (red dots). Isolated molecule (a), single coupled molecule (b) and ensemble of 5 molecules (c). Legends are explained in the main text.

isolated molecule the dissociation probability and linear absorption spectrum remain proportional to each other at all photon energies, indicating that all excited population eventually dissociates. The dissociation probability is defined as $P_{\text{dis}} = \langle \Psi(T) | \hat{\Theta}(R_1 - R_d) | \Psi(T) \rangle$, where $\Theta(x)$

is the Heaviside step function, $R_d = 10$ au and $T = 1$ ps is a sufficiently long final propagation time ensuring that P_{dis} has become stationary.

The photo-dissociation dynamics is significantly changed when the molecules are coupled to the cavity mode. Throughout this work the effective cavity-matter coupling is taken as $g/\omega_c=0.01$, where g was defined around Eq. (3) and can be seen as the rms vacuum electric field amplitude of the cavity mode [3]. This coupling strength is small compared to the single-molecule ultra-strong coupling regime, characterized by a Rabi splitting of the polaritonic energy levels (at zero detuning) $\hbar\omega_R = 2g\mu_{01}$ comparable to the transition energy. The collective Rabi splitting is given by $\hbar\Omega_R = 2g\mu_{01}\sqrt{N}$ [33], where N is the number of coupled molecules and μ_{01} the transition dipole matrix element. For NaI at the Franck-Condon geometry this coupling strength results in $\hbar\Omega_R = 0.13$ eV for $N = 1$ and $\hbar\Omega_R = 0.30$ for $N = 5$. Rabi splittings of this order have been observed experimentally using nano-fabricated cavities with coupled organic dye molecules [10, 12].

In the case of a single molecule coupled to the cavity, the absorption spectrum is shown in the right panel of Fig. (1b). A broad absorption band is found in the energy region of the LPB and a set of discrete absorption peaks are seen in the region of the UPB. These markedly different spectral regions can be explained by the potential energy curves of the lower and upper polaritons obtained by diagonalization of the $\hat{H}_{\text{el}} + \hat{H}_{\text{cav}}$ Hamiltonian as a function of R , which correspond to dissociative and bound potentials, respectively, and are shown in the left panel of Fig. (1b).

Population promoted to the LPB immediately dissociates. Hence, in this spectral region the dissociation probability after laser excitation is proportional to the linear absorption spectrum, as in the isolated molecule case. Note that if the LPB would be bound instead of dissociative, population would remain there until eventually spontaneous emission would occur [7, 10]. Conversely, excitation of the upper polariton by the laser pulse populates a progression of meta-stable vibrational states and the dissociation probability of the molecule within the simulation time of $T = 1$ ps remains zero.

The collective behaviour of a molecular ensemble is investigated now by increasing the number of molecules coupled to the cavity mode for the same single-molecule coupling strength as before. The absorption spectrum and dissociation probability as a function of the laser photon energy are shown in the right panel in Fig. (1c) for $N = 5$ molecules. The absorption spectrum in the lower polariton region features now a broad band with internal structure indicative of the superposition of fast dissociation dynamics along one of the molecular coordinates and bound-type dynamics along the other degrees of freedom. The dissociation probability is still mostly proportional to the absorption spectrum. The dynamics

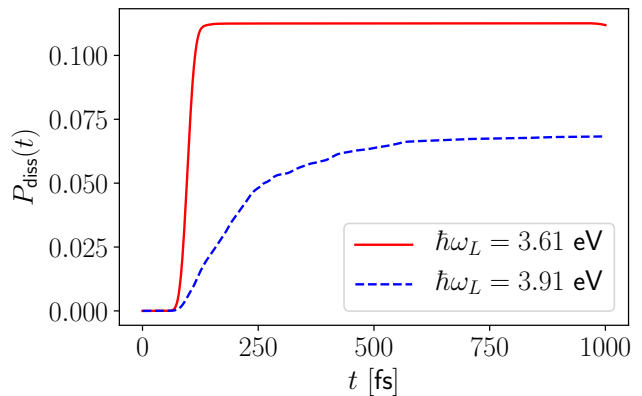


FIG. 2. Single-molecule photo-dissociation probability $P_{\text{dis}}(t) = \langle \Psi(t) | \Theta(R_1 - R_b) | \Psi(t) \rangle$ as a function of time for an ensemble of five molecules interacting with a laser pulse (cf. main text) of photon energy 3.61 eV (red solid curve) and 3.91 eV (blue dashed curve). $R_b = 10$ au.

of the upper polariton however differs from the single-molecule case. The linear absorption spectrum features fewer and broader structures as compared to the vibrational progression of a single coupled molecule and, most remarkably, the probability of dissociation is now comparable to the one in the LPB, although now the splitting between upper and lower polariton has more than doubled by a factor $\sqrt{5}$ as a consequence of the larger collective coupling of the molecules to the cavity.

Since the final dissociation probability in the upper and lower polaritons is now similar, we examine the dynamics of molecular dissociation for two laser photon energies $\hbar\omega_L = 3.61$ and $\hbar\omega_L = 3.91$ eV. These photon energies correspond to the highest dissociation probabilities shown in Fig. (1c) in the LPB and UPB, respectively. Photo-excitation to the lower polariton results in ballistic photo-dissociation, as seen in Fig. (2) by the sudden raise of probability that the wavepacket has propagated beyond $R_d = 10$ au. These dynamics are indicative of unhindered propagation on a dissociative potential. On the other hand, excitation to the upper polariton leads to qualitatively different photo-dissociation dynamics characterized by a slower leakage of the wave packet in about 250 to 500 fs.

In order to understand the origin of these different kinds of dissociative dynamics we direct our attention to the dark states found between the upper and lower polaritons. In the Tavis-Cummings model of an ensemble of two-level atoms coupled to a cavity, and in the zero-detuning case, all dark states are degenerate, appear at the average energy of the two bright polaritons and feature no dipole coupling to the ground state of the hybrid system [2]. Their dark nature is clearly manifest in Fig. (1c) by the practical lack of absorption between 3.65 and 3.85 eV in the linear absorption spectrum. How-

ever, when nuclear motion is present, the degeneracy of the dark states can be lifted through non-adiabatic couplings and a rich structure of collective conical intersections (CCI) emerges. These CCI quickly induce non-radiative decay between the upper and lower polaritons. In the LPB the system can either dissociate, as in the present example with a dissociative molecule, or spontaneously emit a photon if the molecular excited electronic state has a stable molecular geometry.

A cut through the potential energy surfaces obtained by diagonalization of the $\hat{H}_{\text{el}} + \hat{H}_{\text{cav}}$ Hamiltonian in the single-excitation space (SES) and for $N = 5$ is shown in the left panel of Fig. (1c). For five molecules, six polaritonic states are present in the SES, two of which are the bright polaritons and four of them are nominally dark. In the cut shown, $R_2 = R_3 = 5.35$ au, $R_4 = R_5 = 5.5$ au, and R_1 is scanned between 4 and 7.5 au. Two CCI, the origin of which will be discussed below, are seen along this PES cut at precisely $R_1 = 5.35$ and $R_1 = 5.5$, which is not fortuitous.

The matrix representation of the $\hat{H}_{\text{el}} + \hat{H}_{\text{cav}}$ operator in the basis of non-interacting cavity-ensemble states and in the SES results in the molecular Tavis-Cummings Hamiltonian [34]

$$\mathcal{H}_{\text{el-cav}}^{[1]} = \begin{pmatrix} \hbar\omega_c & \gamma^{(1)}(R_1) & \gamma^{(2)}(R_2) & \gamma^{(3)}(R_3) & \dots \\ \gamma^{(1)}(R_1) & \Delta^{(1)}(R_1) & 0 & 0 & \dots \\ \gamma^{(2)}(R_2) & 0 & \Delta^{(2)}(R_2) & 0 & \dots \\ \gamma^{(3)}(R_3) & 0 & 0 & \Delta^{(3)}(R_3) & \dots \\ \vdots & \vdots & \vdots & \vdots & \ddots \end{pmatrix}, \quad (4)$$

where $\Delta^{(\kappa)}(R_\kappa) = V_1^{(\kappa)} - V_0^{(\kappa)}$ is the energy gap of the κ -th molecule and $\gamma^{(\kappa)}(R_\kappa) = g\mu_{01}^{(\kappa)}$ is the effective dipole coupling of the κ -th molecule to the cavity. Hamiltonian (4) has the form of an arrowhead matrix, whose properties are known in the fields of applied mathematics [35, 36] and molecular physics [37].

The most important property of arrowhead matrices for our purposes is the fact that for every m molecules with the same energy gap Δ , there is an eigenvalue $\lambda_j = \Delta$ of multiplicity $m - 1$ [36]. Hence, if two molecules have the same energy gap, there is one eigenstate of the system at the corresponding energy value. In case three molecules have the same energy gap, e.g., molecules 1 to 3, there are two degenerate eigenstates at that energy resulting in a CCI of order two. For the case of identical molecules, this degeneracy is found in the one-dimensional space $R_1 = R_2 = R_3$ and it is lifted by displacements in the two-dimensional branching space that removes this equality. The local symmetry of the identical molecules giving rise to the CCI can be described in the permutation symmetry group S_3 [38], which among others is isomorph with the D_3 point group of an equilateral triangle [39]. As is well known, molecules of D_3

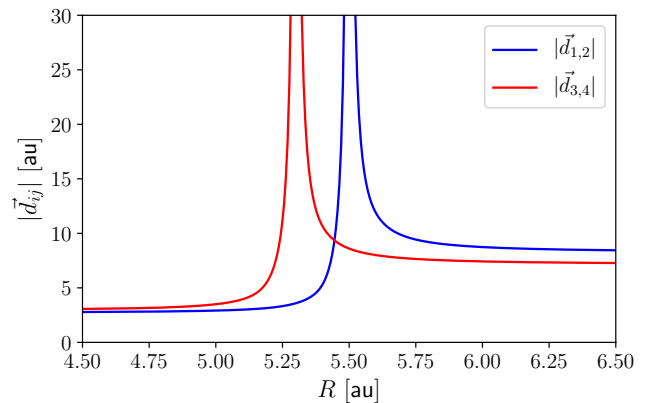


FIG. 3. Absolute value of the non-adiabatic coupling vector $|\langle\psi_i|\vec{\nabla}_R|\psi_j\rangle|$ between crossing pairs of polaritonic states along the same potential energy surface cut of Fig. (1c).

and related symmetry point groups, e.g. C_{3v} , are Jahn-Teller active [39, 40] and the degeneracy of electronic state energies is lifted linearly for displacements out of the highly symmetric atomic arrangement, resulting in conically intersecting potential energy surfaces. Therefore, cavity-induced CCI are, from a mathematical standpoint, analogous to the commonly encountered [41] intramolecular conical intersection case [39, 40, 42–44], with all the consequences for ultrafast non-radiative energy relaxation [44, 45].

Generalising to larger numbers of molecules, the molecular Tavis-Cummings Hamiltonian features a CCI of order $m - 1$ for any subset of m molecules at respective molecular geometries that result in an equal energy gap for all of them. For example, the polaritonic states resulting of four identical molecules with the same geometry can be classified according to the symmetry representations of the S_4 group, which is isomorph with the T_d point group of the tetrahedron and which leads to triply degenerate potential energy crossings and to the $T_2 \otimes t_2$ Jahn-Teller effect [39].

As expected, the non-adiabatic coupling (NAC) vector of CCI diverges to infinity in the same way as for its intramolecular counterparts, which is seen in Fig. (3). There, the absolute value of the NAC vector $|\langle\psi_i|\vec{\nabla}_R|\psi_j\rangle|$ computed numerically is plotted for various pairs of electronic states along the same geometrical cut of Fig. (1c), and the divergence to infinity at the points of CCI is clearly appreciated.

Summarizing, real-time wave packet simulations of a molecular ensemble coupled to a resonance cavity display an ultrafast non-radiative energy relaxation from the upper to the lower polaritonic states. This mechanism is absent for a single coupled molecule *at the same individual coupling strength* to the cavity, and emphasizes the collective nature of the phenomenon. The ultra-

fast non-radiative decay occurs through cavity-induced CCI, which emerge from the arrowhead-matrix form of the molecular Tavis-Cummings Hamiltonian in the SES. Since only the energy gap is determinant for the existence of CCI, these are expected to be robust against molecular rotations or intra-molecular geometrical displacements that modify the effective coupling strength of individual members of the ensemble to the cavity mode, as well as to local interactions with an environment, which will lead only to displacements of the locus of intersection.

O.V. would like to thank Prof. L.S. Cederbaum and Prof. H.-D. Meyer for insightful discussions.

* e-mail: oriol.vendrell@phys.au.dk

- [1] E. T. Jaynes and F. W. Cummings, *Proc. IEEE* **51**, 89 (1963).
- [2] M. Tavis and F. Cummings, *Phys. Lett. A* **25**, 714 (1967).
- [3] S. Haroche and D. Kleppner, *Phys. Today* **42**, 24 (1989).
- [4] R. Miller, T. E. Northup, K. M. Birnbaum, A. Boca, A. D. Boozer, and H. J. Kimble, *J. Phys. B: At Mol Opt Phys* **38**, S551 (2005).
- [5] H. Walther, B. T. H. Varcoe, B.-G. Englert, and T. Becker, *Rep. Prog. Phys.* **69**, 1325 (2006).
- [6] M. Aspelmeyer, T. J. Kippenberg, and F. Marquardt, *Rev. Mod. Phys.* **86**, 1391 (2014).
- [7] D. M. Coles, P. Michetti, C. Clark, W. C. Tsoi, A. M. Adawi, J.-S. Kim, and D. G. Lidzey, *Adv. Funct. Mater.* **21**, 3691 (2011).
- [8] T. Schwartz, J. A. Hutchison, C. Genet, and T. W. Ebbesen, *Phys. Rev. Lett.* **106**, 196405 (2011).
- [9] J. A. Hutchison, T. Schwartz, C. Genet, E. Devaux, and T. W. Ebbesen, *Angew. Chem. Int. Ed.* **124**, 1624 (2012).
- [10] T. Schwartz, J. A. Hutchison, J. Léonard, C. Genet, S. Haacke, and T. W. Ebbesen, *ChemPhysChem* **14**, 125 (2013).
- [11] T. W. Ebbesen, *Acc. Chem. Res.* **49**, 2403 (2016).
- [12] X. Zhong, T. Chervy, L. Zhang, A. Thomas, J. George, C. Genet, J. A. Hutchison, and T. W. Ebbesen, *Angew. Chem. Int. Ed.* **56**, 9034 (2017).
- [13] J. George, S. Wang, T. Chervy, A. Canaguier-Durand, G. Schaeffer, J.-M. Lehn, J. A. Hutchison, C. Genet, and T. W. Ebbesen, *Faraday Discuss.* **178**, 281 (2015).
- [14] J. George, T. Chervy, A. Shalabney, E. Devaux, H. Hiura, C. Genet, and T. W. Ebbesen, *Phys. Rev. Lett.* **117**, 153601 (2016).
- [15] G. Morigi, P. W. H. Pinkse, M. Kowalewski, and R. de Vivie-Riedle, *Phys. Rev. Lett.* **99**, 073001 (2007).
- [16] F. Caruso, S. K. Saikin, E. Solano, S. F. Huelga, A. Aspuru-Guzik, and M. B. Plenio, *Phys. Rev. B* **85**, 125424 (2012).
- [17] J. Galego, F. J. Garcia-Vidal, and J. Feist, *Phys. Rev. X* **5**, 041022 (2015).
- [18] J. Schachenmayer, C. Genes, E. Tignone, and G. Pupillo, *Phys. Rev. Lett.* **114**, 196403 (2015).
- [19] J. A. Ćwik, P. Kirton, S. De Liberato, and J. Keeling, *Phys. Rev. A* **93**, 033840 (2016).
- [20] J. Galego, F. J. Garcia-Vidal, and J. Feist, *Nat. Commun.* **7**, 13841 (2016).
- [21] F. Herrera and F. C. Spano, *Phys. Rev. Lett.* **116**, 238301 (2016).
- [22] M. Kowalewski, K. Bennett, and S. Mukamel, *J. Phys. Chem. Lett.* **7**, 2050 (2016).
- [23] M. Kowalewski, K. Bennett, and S. Mukamel, *J. Chem. Phys.* **144**, 054309 (2016).
- [24] J. Flick, M. Ruggenthaler, H. Appel, and A. Rubio, *Proc. Natl. Acad. Sci.* **114**, 3026 (2017).
- [25] J. Galego, F. J. Garcia-Vidal, and J. Feist, *Phys. Rev. Lett.* **119**, 136001 (2017).
- [26] H. L. Luk, J. Feist, J. J. Toppari, and G. Groenhof, *J. Chem. Theory Comput.* **13**, 4324 (2017).
- [27] O. Vendrell, *Chem. Phys.* **509**, 55 (2018).
- [28] R. Sáez-Blázquez, J. Feist, A. I. Fernández-Domínguez, and F. J. García-Vidal, *arXiv*, 1804.01784 (2018).
- [29] F. H. M. Faisal, *Theory of Multiphoton Processes* (Springer US, 1987).
- [30] A. H. Zewail, *Science* **242**, 1645 (1988).
- [31] U. Manthe, H.-D. Meyer, and L. S. Cederbaum, *J. Chem. Phys.* **97**, 3199 (1992).
- [32] M. H. Beck, A. Jäckle, G. A. Worth, and H.-D. Meyer, *Phys. Rep.* **324**, 1 (2000).
- [33] R. J. Thompson, G. Rempe, and H. J. Kimble, *Phys. Rev. Lett.* **68**, 1132 (1992).
- [34] See supporting Information.
- [35] J. H. Wilkinson, *Oxford: Clarendon Press, 1965* (1965).
- [36] D. O'Leary and G. Stewart, *J. Comput. Phys.* **90**, 497 (1990).
- [37] O. Walter, L. S. Cederbaum, and J. Schirmer, *J. Math. Phys.* **25**, 729 (1984).
- [38] P. R. Bunker and P. Jensen, *Molecular Symmetry and Spectroscopy*, 2nd ed. (NRC Research Press, 1998) p. 747.
- [39] H. Köppel, D. R. Yarkony, and H. Barentzen, eds., *The Jahn-Teller Effect* (Springer Berlin Heidelberg, 2010).
- [40] W. Domcke, D. R. Yarkony, and H. Köppel, eds., *Conical Intersections: Electronic Structure, Dynamics & Spectroscopy* (World Scientific Pub Co. Inc., 2004).
- [41] D. Truhlar and C. Mead, *Phys. Rev. A* **68**, 032501 (2003).
- [42] D. R. Yarkony, *Rev. Mod. Phys.* **68**, 985 (1996).
- [43] D. R. Yarkony, *Acc. Chem. Res.* **31**, 511 (1998).
- [44] G. A. Worth and L. S. Cederbaum, *Annu. Rev. Phys. Chem.* **55**, 127 (2004).
- [45] T. Schultz, J. Quenneville, B. Levine, A. Toniolo, T. J. Martinez, S. Lochbrunner, M. Schmitt, J. P. Shaffer, M. Z. Zgierski, and A. Stolow, *J. Am. Chem. Soc.* **125**, 8098 (2003).